

# Experimental Studies on Spacecraft Arcing

M. R. Carruth Jr.,\* J. A. Vaughn,† and R. T. Bechtel‡  
NASA Marshall Space Flight Center, Huntsville, Alabama 35812  
and  
P. A. Gray§  
Sverdrup Technologies, Huntsville, Alabama 35806

Space Station Freedom (SSF) will be the largest and highest powered spacecraft put into orbit. Because of the balance of leakage currents through the ambient ionospheric plasma, the structure will be driven approximately 140 V negative of the ambient plasma without a plasma contractor for negative control. Surface materials such as anodized aluminum will have the entire voltage dropped across a thin dielectric that may not have sufficient dielectric strength to prevent dielectric breakdown. The results of experiments done to measure the dielectric breakdown threshold of anodized aluminum with a range of anodization thicknesses designed to span a range of thermal control properties being considered for SSF show breakdown thresholds near -90 V in an argon plasma with densities comparable to that of low-Earth orbit. Because of the size of Space Station Freedom, the thin anodization layer can store large amounts of charge. Experiments done to simulate the discharge of these large capacitances indicated currents as large as 1000 A are possible, and observations of the anodization surface show the energy released in these high-current arcs produced craters through the anodic coating to the bare aluminum. The debris from the craters produces a contamination source for sensitive surfaces.

## Introduction

WITH few exceptions, spacecraft flown to date have had power levels under a kilowatt and low voltage distribution systems. Electrical distribution systems have typically been at 28 V, and solar arrays that convert sunlight into electrical power have operated from 30 to 36 V. The highest voltage solar array flown by NASA was Skylab, which had two separate arrays at different voltages. One solar array was approximately 65 V and the other near 90 V.<sup>1</sup> Skylab also had a 28-V secondary distribution system.

It has long been recognized that, for large spacecraft with much higher power levels, it is necessary to operate at much higher voltages. This is necessary to prevent the handling of large currents and to operate efficiently. Therefore, for many years research has been conducted into the interaction of high-voltage solar arrays and power systems with the low-Earth orbit plasma environment.<sup>2-5</sup> These interactions can have a detrimental effect on the lifetimes of spacecraft systems.

A spacecraft immersed in the low-Earth orbit plasma must come to an equilibrium potential such that it collects zero net current. The electrons are very mobile and easy to collect, whereas the ions are massive and are difficult to collect. Therefore, to collect the same current of ions as electrons, most of the exposed spacecraft surface will be negative of the ambient plasma. The ambient plasma is the ultimate local potential reference and is defined as zero volts. When a spacecraft such as Space Station Freedom (SSF), with a solar array generating 160 V, is in orbit, most of this voltage will be negative of the ambient plasma. Laboratory and flight data have shown this to be the case.<sup>6-9</sup> This is a simplified description, and the actual equilibrium potential will depend on solar array design, orientation of the solar array to the spacecraft velocity vector and the sun, and the conducting area on the spacecraft. Tests of a segment of SSF solar array in a vacuum chamber

with a plasma environment have shown that 20-40 V of the 160 V on the array will be positive of the plasma potential and the remainder will be negative.<sup>10</sup> Figure 1 illustrates the relative potentials of the solar array with respect to the plasma as well as the spacecraft structure. For the baseline case of negative ground, the structure will be driven negative of the ambient plasma.

In recent years research has been conducted to examine tailoring anodization coatings on the external skin of the spacecraft for passive thermal control. Skylab, which was the only previous experience with high-powered solar arrays, had an anodic thickness on the order of a few mils,<sup>1</sup> which was not tailored for passive thermal control but corrosion prevention. The thick anodic coating would have prevented detection of any problem with dielectric breakdown. When tailoring the thermal control characteristics (i.e., solar absorptance  $\alpha$  and thermal emittance  $\epsilon$ ) of anodized aluminum, the thermal emittance is directly related to the anodic layer thickness. The thickness of the anodization layer is in turn related to the dielectric breakdown strength. To prevent internal cold spots, the thermal emittance needs to be small, which indicates a thin anodic layer leading to dielectric breakdown.

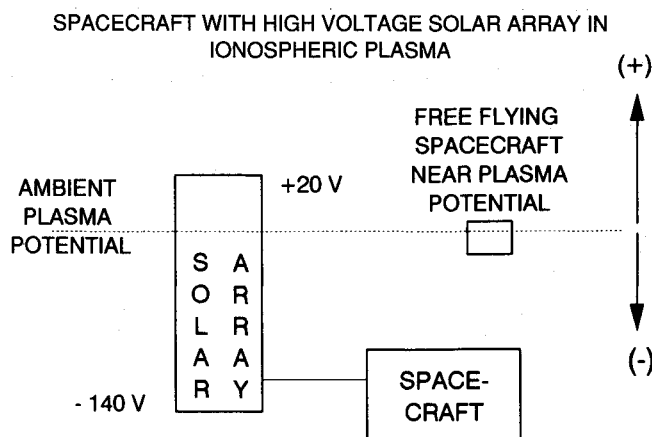


Fig. 1 Diagram of floating potentials relative to ambient plasma potential.

Received Dec. 30, 1991; presented as Paper 92-0820 at the AIAA 30th Aerospace Sciences Meeting and Exhibit, Reno, NV, Jan. 6-9, 1992; revision received June 28, 1992; accepted for publication July 17, 1992. This paper is declared a work of the U.S. Government and is not subject to copyright protection in the United States.

\*Chief, Physical Sciences Branch. Member AIAA.

†Materials Engineer, Physical Sciences Branch.

‡Chief, Electrical Power Branch. Senior Member AIAA.

§Engineer, Materials and Process Department, 620 Discovery Dr.

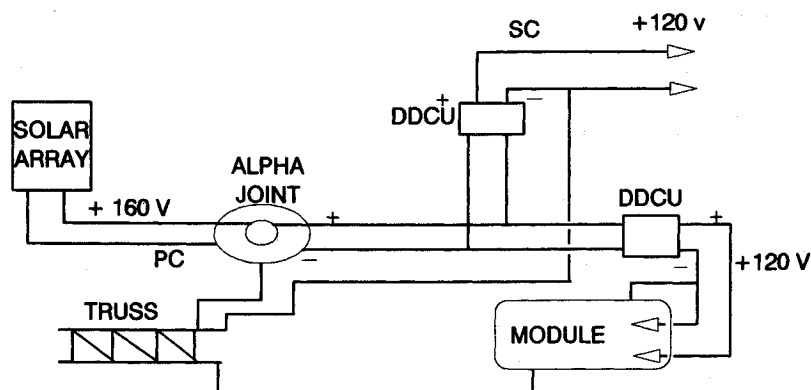


Fig. 2 Schematic of SSF solar array and power distribution negatively grounded to structure.

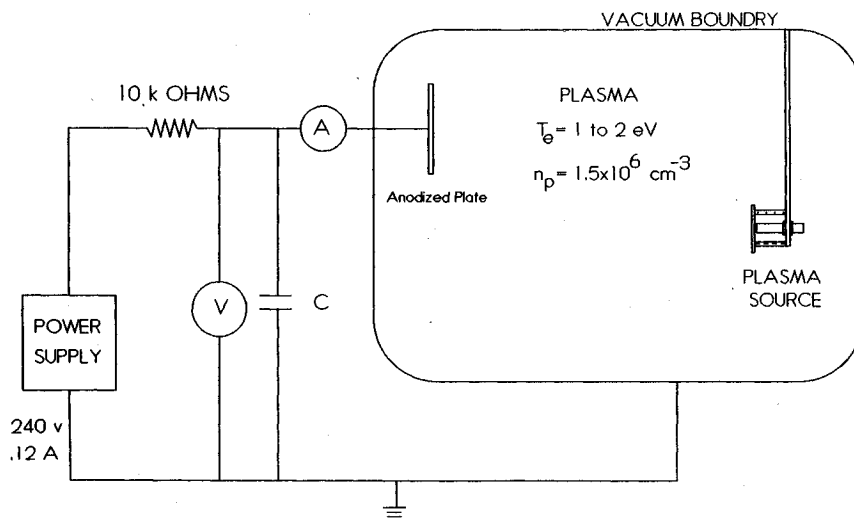


Fig. 3 Electrical breakdown test apparatus.

The thin anodization layer that is a dielectric will store charge similar to a capacitor. Because the anodization layer does not have sufficient dielectric strength to withstand the voltage stress, dielectric breakdown will occur, discharging some or all of the stored charge. The amount of the capacitance discharged is still not understood, but this is a subject of ongoing tests. The discharge of this stored energy affects the surface of the anodization layer and changes the optical properties required for passive thermal control.

### Space Station Freedom Design Issues

The design of the SSF power system has gone through several iterations. Early in the SSF program there were working groups that were addressing the question of SSF interactions with the ambient plasma. When the primary power distribution system was ac, the solar array was to be electrically isolated from the truss and modules. The structure in this case would float near the ambient plasma potential, and the interactions with the plasma would be insignificant.

The ac design was abandoned and a high-voltage dc primary distribution system was adopted during one of the redesign activities. The adoption of the high-voltage dc primary distribution system eliminated the isolation between the SSF structure and the power system. The solar array will operate at a nominal voltage of 160 V, and the power is distributed at this voltage. Dc-to-dc converters isolate the primary distribution from the secondary power distribution in the modules and on the truss. The secondary power distribution is at 120 V dc. The all-dc system assumes a negative ground of the primary and secondary power system to the structure, and this has been baselined for SSF. Figure 2 shows the baseline configuration.

There are various interactions with the ambient plasma that must be considered, but this paper deals only with the issue of dielectric breakdown on SSF surfaces. The outer surfaces of SSF are primarily nonconducting. The outer surface of the truss structure, the outer debris shield, the module surfaces, and the solar array masts are designed to be anodized aluminum.<sup>11,12</sup> The type and thickness of anodization is tailored to provide required emissivity and absorptivity values for thermal control purposes.

To meet the required emissivity values, the anodized layer is approximately 1–5  $\mu$  thick. The structure is at about 140 V negative of the ambient plasma. The surface of the dielectric media will be at plasma floating potential. If the thin anodization layer has insufficient dielectric strength to withstand this voltage level, dielectric breakdown and arcing will result.

The surface area of SSF will be very large. Each full size module will have an exposed surface area of approximately 200 m<sup>2</sup>. The thin anodization layer and the large surface area will provide a

Table 1 Range of anodizing conditions

Test panel sample	Anodizing voltage, V	Anodizing time, min	Sealed/unsealed	Optical properties	
				Absorptance, d	Emittance, $\epsilon$
A	40	30	Sealed	0.38	0.28
B	40	25	Sealed	0.39	0.27
C	40	60	Sealed	0.41	0.65
D	40	30	Unsealed	0.26	0.18
E	40	30	Sealed and aged <sup>a</sup>	0.39	0.27

<sup>a</sup>Aged at 170°F for seven days.

### ARC RATE IN A PLASMA OF CHROMIC ACID ANODIZED ALUMINUM

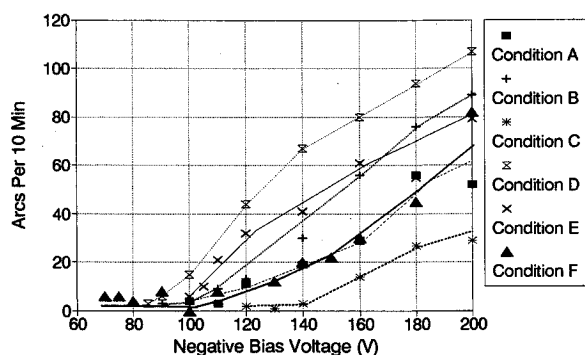


Fig. 4 Chromic acid anodized aluminum arc rate in a plasma.

### BREAKDOWN THRESHOLDS IN A PLASMA Area Effects on Breakdown Threshold

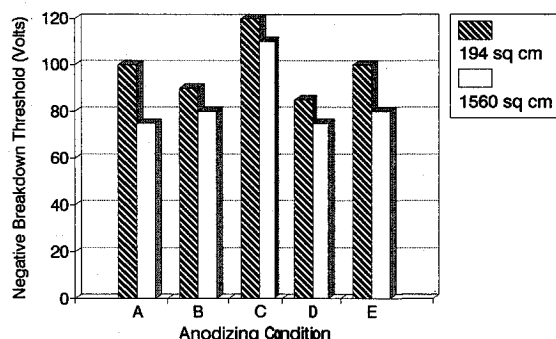


Fig. 5 Effects of area on breakdown voltage.

capacitance on the order of 1000–3000  $\mu\text{F}$ . All SSF structural elements will be connected electrically and will be capable of storing many joules of energy, which may be released through arcs resulting from dielectric breakdown of the anodized surface. The combination of resistances and inductances in the available current closure paths and in the structure will be important in establishing how current may be supplied from the structure on SSF that is remote from an arc site. Only the breakdown voltage and arc characteristics for given capacitances will be addressed herein.

It is important to note that, even if a material has sufficient dielectric strength to prevent electrical breakdown, the energy will still be stored in the SSF capacitance. The increasing presence of micrometeoroid and space debris particles in low-Earth orbit<sup>13</sup> increases the likelihood of a micrometeoroid or debris impact that provides a means of discharging the stored energy. From micrometeoroid and space debris impact testing it is known that at the high-impact velocities the particle vaporizes and ionizes as it penetrates.<sup>14</sup> Very small particles at high velocities will be able to penetrate the thin anodization layer. The resultant plasma from the impact may provide a conducting path to initiate an arc at that site by discharging the SSF capacitance, even if only locally. There are some data to support this scenario, but more data are required.<sup>15,16</sup>

### Experimental Test Apparatus

Figure 3 is a schematic of the plasma test facility at the Marshall Space Flight Center (MSFC) where the electrical breakdown testing was performed. The test facility consists of a large cylindrical diffusion pumped vacuum vessel, a hollow cathode plasma source, and the necessary electronics needed to support testing. The chamber is 1.2 m in diameter and 1.8 m long with two cold trapped diffusion pumps. The vacuum facility is capable of a base pressure of  $1 \times 10^{-7}$  Torr. Because of the gas load required to operate the

plasma source, the operating pressure was in the high  $10^{-5}$  Torr range during testing.

The physical operation of a hollow cathode plasma source that was used in these tests has been described in detail by Siegfried.<sup>17</sup> A hollow cathode plasma source was chosen because of its long life capability and its ability to produce a fairly uniform plasma. Langmuir probe measurements done to characterize the plasma in the chamber showed only a factor of two change in plasma density and a small change in the electron temperature from one end of the vacuum chamber to a point near the plasma source.

The anodized aluminum plates used in these tests were chromic acid anodized according to the standard chromic acid anodizing process, BAC 5884 Type I class 1, at Boeing Aerospace. The range of anodizing conditions, which are listed in Table 1, was designed to produce anodic coatings that span a wide range of thermal control properties. The aluminum plates tested were 6061 aluminum anodized on both sides with physical dimensions of 7.6 cm  $\times$  12.7 cm. This produced a surface area of 194  $\text{cm}^2$  exposed to the plasma. Also, larger plates with a surface area of 1560  $\text{cm}^2$  were tested to examine the effect that area has on electrical breakdown characteristics.

Figure 3 shows the general wiring diagram used to bias the anodized aluminum plate in the plasma. The power supply used to produce the desired negative bias on the plate was isolated from the plate by a 10 k $\Omega$  resistor to prevent current from being supplied to the arc by the power supply. A capacitor was added to the circuit to increase the charge storage capability of the plate to eventually simulate the discharge of capacitances on the order of a single SSF module. No capacitor was used when the arc rate tests were performed because the time required to collect enough charge from the plasma to recharge the plate to the given potential would limit the arc rate and provide erroneous arc rate data. When the current in the arc was being measured, the added capacitance was varied from the self-capacitance of the plate (i.e. 0.3  $\mu\text{F}$ ) to 1210  $\mu\text{F}$ . The larger value is on the order of the capacitance calculated for one SSF module. The ammeter used to measure the arc current discharge was an inductive current probe connected to an oscilloscope. The oscilloscope used during these tests had a frequency response of 100 MHz and was capable of recording hundreds of nanosecond rise times, but the inductive current probe had a frequency response of 15 MHz and peak pulse current limit of 500 A. From test observations, the current probe performed well when the magnitude of the current transients were small. Because the oscilloscope had sufficient frequency response, it was felt that the voltage data would provide more accurate data by differentiating the trace to get the current trace.

### Experimental Results

The tests done to examine the electrical breakdown characteristics (i.e., initial breakdown potential and arc rate) of the anodic coating on SSF were performed by first starting and stabilizing the plasma source over a half-hour period. The plasma conditions

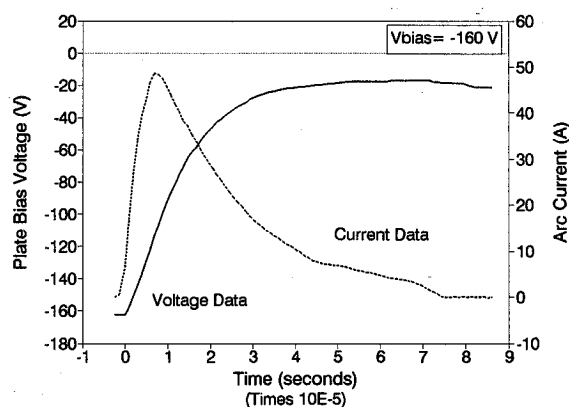


Fig. 6 Typical arc current and voltage data.

# PEAK CURRENTS MEASURED DURING ARC AS A FUNCTION OF EXTERNAL CAPACITANCE

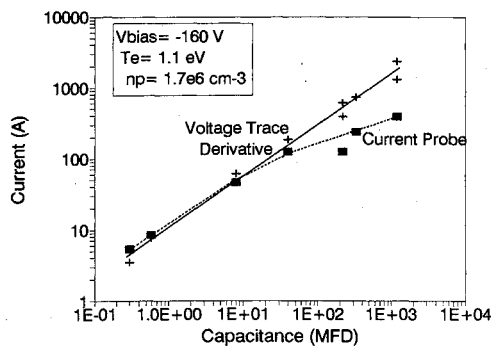


Fig. 7 Comparison of peak current data.

were then measured using a Langmuir probe before beginning the experiment. The anodized aluminum plates were biased starting at a voltage near  $-60$  V. The initial bias was chosen because all samples tested did not produce an arc during a 10-min period. The voltage bias placed on the plate was held for 10 min and the number of arcs counted on a strip chart. The 10-min period was chosen arbitrarily. The factors that contributed to the selection were the need to let the sample remain at voltage for an extended period of time but to be able to complete testing of one sample in a single day. During monitoring of the arc rate the data were easy to decipher because the arc produced large current spikes (i.e., 1-A peaks or larger) during the tests. The voltage was then increased more negative in increments of 5 V and held for 10 min at each condition until a single arc was detected. The voltage bias on the plate where a single arc was observed was considered the breakdown threshold for that sample. After the breakdown threshold was observed, the voltage was increased more negative at a faster rate until the plate was tested at a bias potential of  $-200$  V, which is beyond the expected voltage stress across the anodization layer of SSF.

Figure 4 shows the number of arcs recorded in the 10-min test period as a function of the negative bias voltage applied to the plate. The initial breakdown voltage of all of the plates tested was below the predicted floating potential of SSF (i.e.,  $-140$  V) with the worst test sample being the aluminum plates anodized according to condition D. Also, the number of arcs observed at  $-140$  V was greater than 20 for all but the sample with the thickest anodic layer. The aluminum samples anodized according to conditions A and C bracket the emissivity and absorptivity values required to control the temperature of SSF. Because all of the data shown in this figure were recorded for the one sample size, tests were performed to look at area dependence of the electrical breakdown characteristics.

The results of the tests performed to examine the area dependence of the electrical breakdown characteristics are shown in Fig. 5, which is a bar chart comparing the initial breakdown voltage of the two different size plates at each anodization condition. The test data show that, as the size of the plate increases, the initial breakdown voltage decreases negatively, making it easier to produce an arc at the  $-140$ -V design potential. Also, the increase in area causes more arcs to occur in the 10-min period at any one given bias potential. This fact may be because the number of defects in the anodic coating will increase with surface area, causing an increase in the arc rate, although a definitive explanation is not yet known.

The magnitude of the current transient caused by one of these arcs is also a concern because of the possibility of electromagnetic interference (EMI) effects. Tests to measure the amount of current

in the arc were performed in the same test chamber and configuration as shown in Fig. 3. The plates were biased to  $-160$  V, and current and voltage data were measured as a function of time. Figure 6 shows a typical set of current and voltage traces. This particular set of current and voltage data was measured with  $8 \mu\text{F}$  of additional capacitance to the system. Data of this type were recorded at capacitance levels ranging from  $0.3$  to  $1210 \mu\text{F}$ . From these data traces the charge was calculated by integrating the current trace and comparing it with the charge stored at  $160$  V in the particular capacitor to account for all of the charge in the system. Also, the voltage traces were numerically differentiated to compare the calculated current data with the current data measured with the current probe.

Figure 7 compares the peak currents measured during the arcing experiments plotted on a log-log scale. The data in this figure are shown for two reasons: 1) to demonstrate the problems encountered using the inductive current probe to measure current transients of this magnitude and 2) to provide an indication of the current magnitude possible under the current grounding design. The data measured with the inductive current probe begin to differ from the current data calculated from the voltage trace at the higher current levels, near  $150$  A. The cause for the difference is because the inductive current probe did not have the time response to respond to the large current transients in the time required, a  $5$ – $10 \mu\text{s}$  rise time. The oscilloscope was able to capture the voltage data accurately to provide the best measure of the current transients at the higher current levels. Previously, the capacitance of a single SSF module was stated as  $1000 \mu\text{F}$ . From the data of Fig. 7, a capacitance level of  $1000 \mu\text{F}$  would produce a current of  $1500$  A assuming the entire module would discharge at once. However, there is some question whether the entire module would discharge at once. Testing is ongoing in this lab to see if the low-Earth orbit plasma environment will be able support a transient of this magnitude. Even if only a fraction of the capacitance can discharge during one arc, current levels on the order of several hundred amperes are possible.

Figure 8 is a photograph taken with a light-sensitive high-speed video camera of a single arc. The videotape from the camera can be stepped through frame by frame and any particular frame downloaded to a computer for printing. In the photograph, the small circle of light in the lower left-hand corner is the light produced by the plasma source. The arc is the large burst of light seen in the upper right-hand corner of the picture. The streaks of light originating in the arc were identified as particles of the anodized plating and aluminum from the plate. The outline of the plate can be seen behind the arc flash. Arcs of this magnitude will change surface properties and can cause EMI problems. Particles ejected from the bulk material during the arc will be a source of contamination.

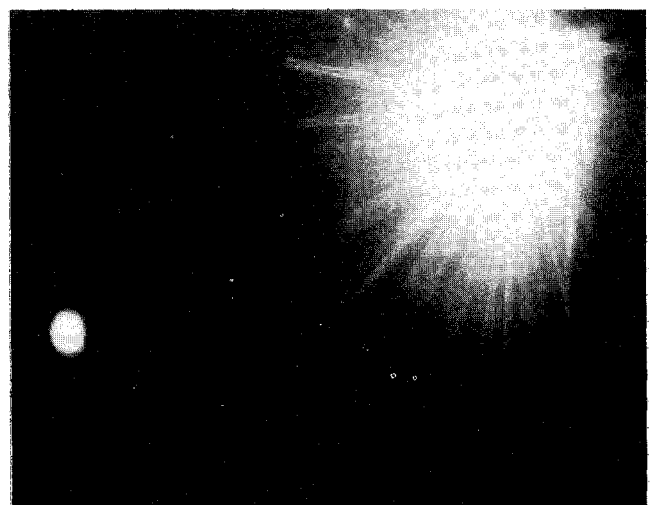


Fig. 8 Photograph of a single arc.

## Conclusions

With the baseline of negative ground on SSF, the structure can be at a high negative voltage relative to the ambient plasma. The data collected using aluminum plates prepared with candidate anodization procedures, which provide a range of acceptable thermal properties, show that dielectric breakdown will occur without active control of potentials. Only two sizes of anodized plates were tested in the plasma environment, but a definite trend of lower dielectric breakdown voltage with increased area was noted. It is possible that this trend was due to the anodic layer thickness variation inherent in processing large panels. Also, it is anticipated that, if the bias voltage is low enough, even the thinnest anodization layer should be able to prevent breakdown, providing a limit to how low the breakdown threshold can go. Even if a material were used that met all other requirements and had sufficient dielectric strength to withstand the voltage drop from the structure to the ambient plasma potential, the possibility of arc initiation due to debris impacts is real. Studies in this area are required to quantify the conditions under which this could occur.

The ability of the stored charge to be released through the arc will depend on the closure of the current paths from the arc into the plasma and through the structure. The resistance and inductance effects of the structure and current paths will be important. Study of these effects is beyond the scope of this paper. However, arc data with charged capacitors having an energy release that can reasonably be expected in an arc on SSF modules show that very large peak currents, on the order of hundreds of amperes, with fast rise times are possible. Pitting and removal of the anodized surface will result, producing undesirable effects such as contamination, changing thermal properties, current and voltage transients and EMI. There are numerous design solutions that can alleviate these problems. The design solution includes both active and passive solutions. SSF has baselined a plasma contactor to control the potentials, thus eliminating the arcing problem.

## References

<sup>1</sup>Bechtel, R. T., private communication, NASA Marshall Space Flight Center, Electrical Division, Huntsville, AL, 1991.

<sup>2</sup>Kennerud, K. L., "High Voltage Array Experiments," NASA CR-121280, 1974.

<sup>3</sup>Stevens, N. J., "Investigation of High Voltage Spacecraft System Interactions with Plasma Environments," AIAA Paper 78-672, 1978.

<sup>4</sup>McCoy, J. E., and Konradi, A., "Sheath Effects Observed on a 10 Meter High Voltage Panel in Simulated Low Earth Orbit Plasmas," *Spacecraft Charging Technology-1978*, NASA CP-2071, Nov. 1978, pp. 315-340.

<sup>5</sup>Grier, N. T., and Stevens, N. J., "Plasma Interaction Experiment (PIX) Flight Results," *Spacecraft Charging Technology-1978*, NASA CP-2071, Nov. 1978, pp. 295-314.

<sup>6</sup>Grier, N. T., "Experimental Results on Plasma Interactions with Large Surfaces at High Voltages," NASA TM-81423, 1980.

<sup>7</sup>Grier, N. T., "Plasma Interaction Experiment II (PIX-2): Laboratory and Flight Experiment Results," *Spacecraft and Environmental Technology-1983*, NASA CP-2359, Oct. 1983, pp. 333-348.

<sup>8</sup>Jones, S., Stakus, J., and Byers, D., "Preliminary Results of Sert II Spacecraft Potential Measurements Using Hot Wire Emissive Probes," AIAA Paper 70-1127, 1970.

<sup>9</sup>Kerslake, W., and Domitz, S., "Neutralization Tests on the Sert II Spacecraft," AIAA Paper 79-2064, 1979.

<sup>10</sup>Felder, M., private communication, NASA Lewis Research Center, Cleveland, OH, 1991.

<sup>11</sup>Sudduth, R., private communication, Boeing Aerospace Co., Huntsville, AL, 1991.

<sup>12</sup>Nahra, H., private communication, NASA Lewis Research Center, Cleveland, OH, 1991.

<sup>13</sup>Kessler, D. J., Reynolds, R. C., and Anz-Meador, P. D., "Orbital Debris Environment for Spacecraft Designed to Operate in Low Earth Orbit," NASA TM-100471, April 1989.

<sup>14</sup>Anderson, C. E., Jr., Trucano, T. G., and Mullin, S. A., "Debris Cloud Dynamics," *International Journal of Impact Engineering*, Vol. 9, No. 1, 1990, pp. 89-113.

<sup>15</sup>Schneider, E., "Micrometeorite Impact on Solar Panels," *Photovoltaic Generators in Space*, European Space Agency, ESA SP-267, The Hague/Scheveningen, The Netherlands, Oct. 1986, pp. 171-174.

<sup>16</sup>Weishaupt, U., Kuczera, H., and Roit, M., "Micrometeorite Exposure of Solar Arrays, *Photovoltaic Generators in Space*, European Space Agency, ESA SP-267, The Hague/Scheveningen, The Netherlands, Oct. 1986, pp. 175-180.

<sup>17</sup>Siegfried, D. E., "A Phenomenological Model for Orificed Hollow Cathodes," NASA CR-168026, Dec. 1982.

Alfred L. Vampola  
Associate Editor